

No. AT(30-1)-2098.

†Present address: Kobenhavns Universitet, Niels Bohr Institutet, Copenhagen, Denmark.

<sup>1</sup>K. Bleuler and C. Terreaux, *Helv. Phys. Acta* **30**, 183 (1957).

<sup>2</sup>J. P. Amiet and P. Huguenin, *Nucl. Phys.* **46**, 171 (1963).

<sup>3</sup>J. P. Amiet and P. Huguenin, *Nucl. Phys.* **80**, 353 (1966).

<sup>4</sup>W. Ebenhöh, *Z. Physik* **195**, 171 (1966).

<sup>5</sup>W. H. Bassichis, A. K. Kerman, and J. P. Svenne, to be published. For an exposition of the Hartree-Fock

method see M. Baranger, *Cargèse Lectures in Theoretical Physics* (W. A. Benjamin, Inc., New York, 1963).

<sup>6</sup>F. Tabakin, *Ann. Phys. (N.Y.)* **30**, 51 (1964).

<sup>7</sup>M. H. Hull and C. M. Shakin, *Phys. Letters* **19**, 506 (1965).

<sup>8</sup>T. Hamada and I. D. Johnston, *Nucl. Phys.* **34**, 382 (1962).

<sup>9</sup>C. Bressel, thesis, Massachusetts Institute of Technology (unpublished); C. Bressel, A. Kerman, and E. Lomon, *Bull. Am. Phys. Soc.* **10**, 584 (1965).

<sup>10</sup>F. Villars, private communication.

## ETA PHOTOPRODUCTION IN THE REGION FROM THRESHOLD TO 940 MeV\*

R. Prepost, D. Lundquist, and D. Quinn

High-Energy Physics Laboratory and Department of Physics, Stanford University, Stanford, California

(Received 21 November 1966)

We have measured the photoproduction of the  $\eta^0$  meson in the region from threshold to ~940 MeV. The differential cross section near 90° in the center of mass is characterized by a rapid rise near threshold reaching a maximum value of ~1  $\mu\text{b}/\text{sr}$  approximately 40 MeV above threshold. The cross section then decreases to a value of 0.3  $\mu\text{b}/\text{sr}$  at a laboratory photon energy of ~900 MeV. Several different angles have been measured at a laboratory photon energy of 790 MeV and the angular distribution is consistent with isotropy. This implies either an S or P wave with  $T = \frac{1}{2}$ ,  $J = \frac{1}{2}$  near threshold. Recent phase-shift analyses of pion-nucleon scattering suggest that the  $\eta^0$  production near threshold is to be identified with the  $N_{1/2}^*(1550 \text{ MeV}) S_{11}$  state.

Photoproduction cross-section measurements of the eta, a pseudoscalar meson with positive G parity and mass  $548.6 \pm 0.4 \text{ MeV}$ , have previously been obtained at higher photon energies than the range covered by this experiment.<sup>1</sup> More recently, the Frascati group has extended its measurements to lower energies and there is thus some overlap between the present experiment and the Frascati results.<sup>2</sup> In addition, there are new data in the region from 950-1100 MeV from Heusch et al.<sup>3</sup> However, all these previous experiments measure the  $\eta^0$  production for decay into a specific channel, viz.,  $\eta^0 \rightarrow \gamma + \gamma$ . Comparison with the present results thus requires a knowledge of  $\Gamma_{\gamma\gamma}/\Gamma_{\text{total}}$ , the branching ratio for the two-photon decay mode as compared with all other channels.

Observation of  $\eta^0$  photoproduction in the re-

action  $\gamma + p \rightarrow \eta^0 + p$  has been accomplished by using counter techniques with the Stanford Mark III 1.1-BeV linear electron accelerator.<sup>4</sup> Since this process has a two-body final state, a measurement of the proton angle and momentum is sufficient to determine uniquely the incident photon energy.

The experimental set up consists of equipment as follows: The linac electron beam is brought out into the experimental area and passes through two secondary emission monitors which are used to integrate the electron-beam current. These are followed by an air Čerenkov counter used to monitor the beam pulse shape. The electron beam is then incident upon a radiator foil typically ~0.01 radiation lengths to produce the photon beam. The photon and electron beam then pass through a sweeping magnet which deflects the electron beam away from the target. The photon beam then passes through a liquid hydrogen target.

The recoil protons are detected by counters at the exit focus of a 44-in. radius, 90° bend,  $n=0$  magnet which has 0.1% momentum resolution up to 700 MeV/c. The detecting counters consist of three backing counters and seven momentum-defining counters which are 1% in momentum width. The pulse-height distributions of the backing counters were carefully monitored and used to reject coincidences due to  $\pi^+$  and  $e^+$ . The momentum defining counters are oriented in the focal plane of the spectrometer such that they are parallel to lines of constant photon energy for the reaction under investigation.

Thus, for a particular momentum and angle setting of the spectrometer, the proton yields will increase as the bremsstrahlung end point energy is raised step by step across the threshold for a new process. In particular, if the new process has a two-body final state, the proton yield as a function of electron energy will trace out a characteristic bremsstrahlung curve for a fixed photon energy and variable end-point energy. The energy resolution of the momentum defining counters was between 5 and 10 MeV for most of the experimental points. This narrow energy resolution enhances the sensitivity enough to see steps in the proton yield.

Recoil protons at fixed angle and fixed momentum with a bremsstrahlung photon beam may be produced from several different reactions. The processes which produce significant backgrounds for this experiment are

$$\gamma + p \rightarrow \pi^0 + p \quad (1)$$

and

$$\gamma + p \rightarrow \pi^+ + \pi^- + p. \quad (2)$$

Both these backgrounds have lower laboratory threshold energies than  $\gamma + p \rightarrow \eta^0 + p$ ; thus the proton yield at bremsstrahlung end-point energies which are high enough to produce the  $\eta^0$  will have a significant background contribution from processes (1) and (2). The technique used in this experiment has been to trace out the proton yield all the way from  $\pi^0$  threshold to 150 MeV above the kinematic threshold for  $\eta^0$  production for each momentum-angle setting of the spectrometer. The  $\pi^0$  and pion-pair yields below  $\eta^0$  threshold were fitted to simple approximations for the shape of the pion-pair yield and single  $\pi^0$  photoproduction, and the fits were used to subtract these backgrounds above the kinematic threshold for  $\eta^0$  production.

Figures 1(a)-1(c) show typical yield curves. For fixed spectrometer momentum and angle, the photon energy and center-of-mass angle for the  $\eta^0$  differential cross-section measurement is uniquely determined. As the accelerator energy is increased step by step, the first noticeable threshold is single  $\pi^0$  production via  $\gamma + p \rightarrow \pi^0 + p$  (the cross section for  $\gamma + p \rightarrow \gamma + p$  is too small to be seen against the larger  $\pi^0$  signal). If no other production channels opened up, the proton yield would flatten off some 40 MeV above the  $\pi^0$  threshold and remain approximately constant with increased energy. The

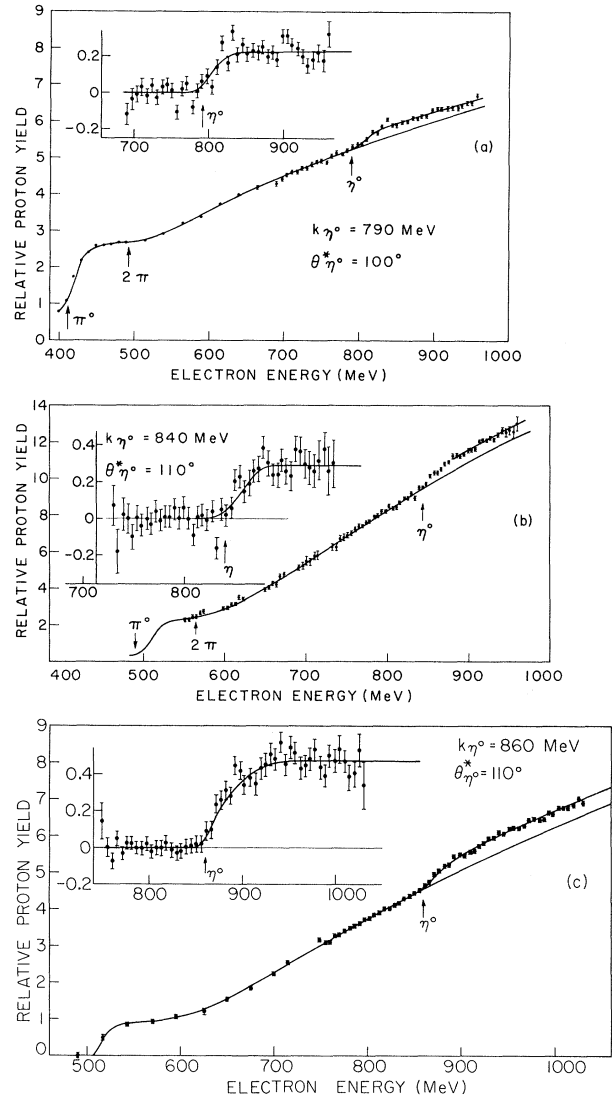


FIG. 1. Three typical proton-yield curves at fixed spectrometer momentum and angle showing (a)  $\pi^0$  threshold, (b) two pion production, and (c) the  $\eta^0$  step. The insert in the upper left-hand corner shows the same data in the region of  $\eta^0$  production with the  $\pi^0$  and two-pion contributions subtracted, leaving only a yield from  $\eta^0$  production.

next kinematically allowed process is  $\gamma + p \rightarrow \pi^+ + \pi^- + p$ . However, this process has a three-body final state, and therefore the proton yield as a function of bremsstrahlung end-point energy is no longer characteristic of a process with a two-body final state, but traces out a yield which is an integral over photon energies from threshold to the bremsstrahlung end-point energy. This two-pion yield is the major background upon which the  $\eta^0$  signal sits. The  $\eta^0$  production appears as an increase in yield with

the same shape as the  $\pi^0$  yield and rises above a proton background from two-pion and single-pion production. For the experimental points measured, the  $\eta^0$  threshold is generally some 400 MeV above the  $\pi^0$  threshold. Figures 1(a)-1(c) show this expected step at the expected  $\eta^0$  threshold very clearly. The arrows indicate the predicted threshold energy. The yield shows the expected behavior of the bremsstrahlung function, which is characterized by a leveling off of the yield for the new channel some 30-40 MeV above its threshold energy.

In order to determine the  $\eta^0$  production cross section from the yield curves, the height of the proton step must be determined. It is therefore necessary to extrapolate the two-pion and  $\pi^0$  yields from below the  $\eta^0$  threshold where they are measured directly to above the  $\eta^0$  threshold where the yields are the sum of an  $\eta^0$  signal plus the two-pion and  $\pi^0$  signals. We have used several procedures to make this extrapolation. We have found that both pure phase space and a linear function give a good fit to the shape of the two-pion yield in the vicinity of the  $\eta^0$  threshold. The actual interval which is fit is the region 100 MeV below the  $\eta^0$  threshold and a 100-MeV interval which starts 50 MeV above the  $\eta^0$  threshold. In Figs. 1(a)-1(c) the solid line is drawn to represent the actual least-squares curve. In this manner we obtain a least-squares solution for the height of the  $\eta^0$  step.

The inserts in Figs. 1(a)-1(c) show the proton yields in the vicinity of the  $\eta^0$  threshold with the background processes subtracted. These background processes include single-pion production, two-pion production, and small (<10%) empty target background. The two-pion yield has been fit with a pure phase-space function. If the background has been subtracted properly, the remaining yield will have the shape of a bremsstrahlung curve for fixed photon energy. This yield must become approximately constant some 50 MeV above the threshold. Figures 1(a)-1(c) showing the subtracted yields have this feature as do our other yield curves. This gives us a direct check that the two-pion fit is a valid representation for the two-pion yield.

We have measured such yield curves for a range of photon energies from 20 MeV above the  $\eta^0$  threshold to ~940 MeV in approximately 25-MeV intervals at  $\eta^0$  center-of-mass angles ranging from 110° to 90°. The angular dis-

tribution was taken at 790-MeV laboratory photon energy. The center-of-mass angles measured at this energy are 140°, 100°, 110°, and 40°. The region away from 90° in the center of mass becomes difficult to measure, since these backward and forward angles correspond to nonideal kinematic conditions or a large  $\pi^0$  proton background from single  $\pi^0$  production. The statistical error on the individual points in the yield curves varies from 0.7-1.0%.

The  $\eta^0$  yields are converted into a differential cross section by normalizing to the proton yield where only  $\pi^0$  protons are produced, keeping the spectrometer momentum and angle fixed. We have then used the available  $\pi^0$  differential cross sections to normalize the data. The available cross-section data have been compiled by Berkelman and Waggoner, and Salin.<sup>5</sup> There are also more recent results obtained by Bacchi.<sup>6</sup> Since  $\pi^0$  measurements do not exist for the exact conditions of some of our data points, we have used the polynomial coefficients as tabulated in Ref. 5 to estimate a  $\pi^0$  cross section. We have assigned an error to the  $\pi^0$  differential cross sections corresponding to the errors on the polynomial coefficients or quoted cross-section errors where direct measurements are available. For most of the  $\eta^0$  differential cross sections this contributes a significant part of the error we have assigned to the  $\eta^0$  cross section. Furthermore, the normalization procedure could lead to systematic errors, quite apart from any errors in the measured yields and background subtractions.

The results are shown in Figs. 2(a) and 2(b). In Fig. 2(a), the differential cross section around 90° in the center of mass is plotted as a function of laboratory photon energy. The original Frascati points and the more recent Frascati and California Institute of Technology<sup>7</sup> points are also shown for reference. These other measurements for the two-photon decay mode of the  $\eta^0$  require a knowledge of  $\Gamma_{\gamma\gamma}/\Gamma_{\text{total}}$  for comparison with this experiment. In particular, the Frascati and California Institute of Technology experiments measure

$$\left. \frac{d\sigma}{d\Omega} \right|_{\eta^0 \rightarrow \gamma + \gamma} = \left. \frac{d\sigma}{d\Omega} \right|_{\text{total}} \frac{\Gamma_{\gamma\gamma}}{\Gamma_{\text{total}}}.$$

We have used the currently accepted branching ratio of the two-photon mode ( $0.33 \pm 0.02$ )<sup>8</sup> in order to convert all experiments to a common cross section. The horizontal flags on the da-

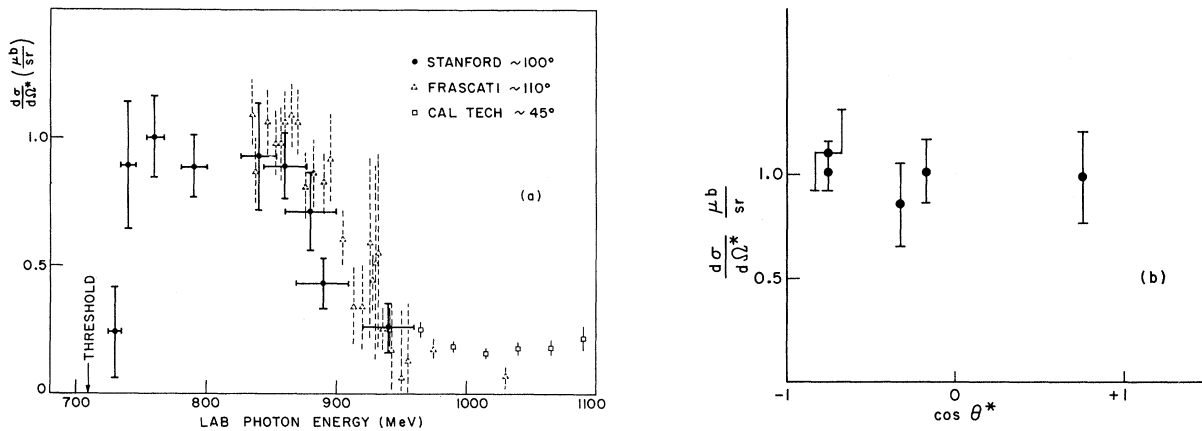


FIG. 2. (a) Differential cross section for  $\gamma + p \rightarrow \eta^0 + p$  showing the results of the present experiment around  $100^\circ$  in the center of mass and the data of Frascati and California Institute of Technology. The California Institute of Technology data are around  $45^\circ$  center-of-mass angle. All results have been reduced to  $(d\sigma/d\Omega^*)_{\text{total}}$ , the center-of-mass differential cross section for  $\eta^0$  production with  $\eta^0 \rightarrow$  all decay modes. The horizontal flags for the present experiment represent the energy interval over which the cross section is averaged. (b) Differential cross section for  $\gamma + p \rightarrow \eta^0 + p$  at 790-MeV laboratory photon energy versus the cosine of the center-of-mass meson angle.

ta points indicate the energy interval over which the cross section is averaged. Figure 2(b) shows the results of the angular distribution at 790 MeV.

The results of the present experiment may be characterized by the following remarks:

(1) The cross section rises rapidly near threshold reaching a maximum value of  $\sim 1 \mu\text{b/sr}$  by 760 MeV. The threshold for  $\eta^0$  production is  $\sim 710$  MeV. This same feature is seen in  $\eta^0$  production via the process  $\pi^- + p \rightarrow \eta^0 + n$ .<sup>9</sup>

(2) The present experiment gives

$$\frac{d\sigma/d\Omega^*|_{\pi^0}}{d\sigma/d\Omega^*|_{\eta^0}} \simeq 4$$

in the photon energy range 760-800 MeV around  $90^\circ$  in the center of mass. At 760 MeV this result is inconsistent with the hypothesis that all the  $\eta^0$  yield near threshold comes from the  $D_{3/2} N^{**}(1512 \text{ MeV})$  simply on the basis of the relative size of the  $D$ -wave angular-momentum barrier for  $\pi^0$  vs  $\eta^0$  production and on the assumption that the  $\eta^0$  nucleon and  $\pi^0$  nucleon couplings are approximately equal.

(3) The angular distribution near threshold, although containing only four points, also tends to rule out pure  $D$ -wave production of the  $\eta^0$ , since this requires  $2 + 3 \sin^2 \theta^*$  for the angular distribution. Our results are consistent with an isotropic angular distribution.

(4) This suggests  $S$ - and/or  $P$ -wave  $J = \frac{1}{2}$  pro-

duction for the  $\eta^0$  near threshold. The most likely candidate is the  $S_{11}(1550)$  resonance, as has been pointed out by several authors for the corresponding case of  $\pi^- + p \rightarrow \eta^0 + n$  near threshold.<sup>10</sup> This resonance has been shown to be highly inelastic in pion-nucleon scattering phase-shift analyses, and simple  $S$ -wave Breit-Wigner resonance formulas plus suitable admixtures from  $P$  and  $D$  partial waves have been successful in fitting the experimental data.

\*Work supported in part by the U. S. Office of Naval Research, Contract No. Nonr 225(67).

<sup>1</sup>C. Bacci, G. Penso, G. Salvini, A. Wattenberg, C. Mencuccini, R. Querzoli, and V. Silvestrini, Phys. Rev. Letters **11**, 37 (1963).

<sup>2</sup>C. Bacci et al., Phys. Rev. Letters **16**, 157, 384(E) (1966).

<sup>3</sup>C. A. Heusch, C. Y. Prescott, E. D. Bloom, and L. S. Rochester, Phys. Rev. Letters **17**, 573 (1966).

<sup>4</sup>A preliminary account of this work is given in *Electron and Photon Interactions at the High Energies, Invited Papers Presented at the International Symposium, Hamburg, 1965* (Springer-Verlag, Berlin, Germany, 1965), Vol. II, p. 152.

<sup>5</sup>K. Berkelman and J. Waggoner, Phys. Rev. **117**, 1364 (1960); Ph. Salin, Nuovo Cimento **28**, 1294 (1963).

<sup>6</sup>C. Bacci et al., *Electron and Photon Interactions at the High Energies, Invited Papers Presented at the International Symposium, Hamburg, 1965* (Springer-Verlag, Berlin, Germany, 1965), Vol. II, p. 232.

<sup>7</sup>The California Institute of Technology data are tak-

en at  $45^\circ$  in the center-of-mass system and there is reason to believe that the angular distribution is not isotropic in this photon energy range, since the angular distributions for  $\pi^- + p \rightarrow \eta^0 + n$  show a distinct anisotropy in the corresponding center-of-mass energy range. [See W. B. Richards *et al.*, Phys. Rev. Letters **16**, 1221 (1966)]. Thus the presentation of the eta photoproduction data from various experiments on a common graph should be considered with this in mind.

<sup>8</sup>A. H. Rosenfeld *et al.*, University of California Radiation Laboratory Report No. UCRL-8030 (revised), 1966 (unpublished).

<sup>9</sup>F. Bulos *et al.*, Phys. Rev. Letters **13**, 486 (1964).

<sup>10</sup>See, for example, A. W. Hendry and R. G. Moorhouse, Phys. Letters **18**, 171 (1965); James S. Ball, Phys. Rev. **149**, 1191 (1961); F. Uchiyama-Campbell and R. K. Logan, Phys. Rev. **149**, 1220 (1966); and Shigeo Minami, Phys. Rev. **147**, 1123 (1966).

## OBSERVATION OF A BACKWARD PEAK IN THE REACTION $\pi^- + p \rightarrow Y^0 + K^0$ AT 6 GeV/c †

David J. Crennell, George R. Kalbfleisch, Kwan Wu Lai, J. Michael Scarr,  
Thomas G. Schumann, Ian O. Skillicorn, and Medford S. Webster  
Brookhaven National Laboratory, Upton, New York  
(Received 9 December 1966)

Recent large-angle  $\pi^\pm p$  elastic scattering experiments in the region of  $\sim 4$  to 8 GeV/c have revealed the existence of a backward peak in the  $\pi^\pm$  angular distributions.<sup>1</sup> This striking feature in the elastic scattering has motivated our search for similar phenomena in other two-body final states, in particular, the final states involving associated production from  $\pi^- p$  interactions.<sup>2</sup>

In this Letter we report the observation of a backward peak in the  $Y^0 K^0$  final state at 6 GeV/c where  $Y^0$  is either  $\Lambda^0$  or  $\Sigma^0$ . The slope of this backward peak is fitted by  $\exp[\gamma_b(u-u_0)]$ , and a value of  $\gamma_b = 5.7 \pm 2$  GeV<sup>-2</sup> is obtained, where  $u$  is the square of the four-momentum transfer in the appropriate crossed channels and  $u_0$  is the kinematic maximum value of  $u$ . We have also obtained a value of the slope for the forward peak,  $\gamma_f = 7.8 \pm 0.5$  GeV<sup>-2</sup>, from an  $\exp[\gamma_f(t-t_0)]$  fit, where  $t$  is the usual square of the four-momentum transfer for the direct channel and  $t_0$  is the kinematic maximum value of  $t$ .

The data were obtained from the Brookhaven National Laboratory 80-inch liquid-hydrogen bubble chamber. The events in which either  $K_1^0 \rightarrow \pi^+ + \pi^-$  or  $\Lambda^0 \rightarrow \pi^- + p$  or both occur in the chamber are used. Events with or without a visible  $\Lambda^0$  are frequently ambiguous between  $\Sigma^0$  and  $\Lambda^0$  hypotheses, since the energy and momentum carried by the  $\gamma$  ray from  $\Sigma^0$  decay are compatible with the uncertainties (such as the uncertainty in beam momentum) at this high energy.<sup>3</sup> We do not therefore make a distinction between these two hypotheses and group them together as  $Y^0$  in the subsequent analysis. The numbers of events found are as fol-

lows:

$$\pi^- + p \rightarrow Y^0 + K^0$$

$$\text{(with both visible), } 143 \text{ events; } \quad (1)$$

$$Y^0(K) \text{ (with } \Lambda^0 \rightarrow \pi^- + p), 217 \text{ events; } \quad (2)$$

$$K^0(Y) \text{ (with } K_1^0 \rightarrow \pi^+ + \pi^-), 88 \text{ events. } \quad (3)$$

Figure 1 is the uncorrected  $\cos\theta_{K^0}$  distribution of  $K^0$ 's in the center-of-mass system. Almost all of the events are found in the forward peak, but there is a well-defined backward peak comprised of ten events<sup>4</sup> in the region of  $\cos\theta_{K^0} < -0.9$ . It is interesting to note that there are only seven events from  $\cos\theta_{K^0} = +0.5$  to

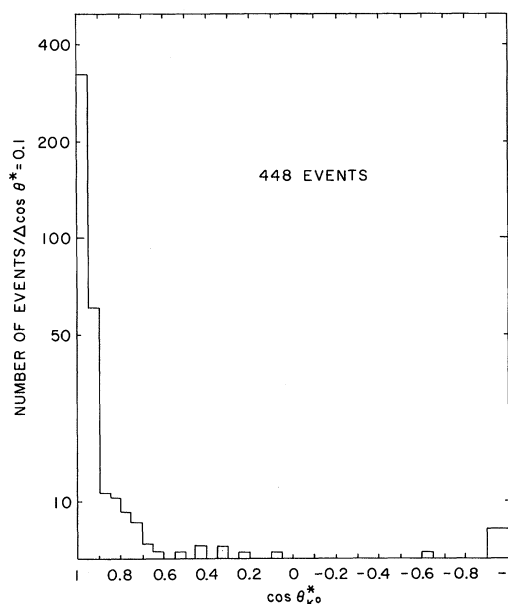


FIG. 1. Uncorrected distribution in  $\cos\theta$  of  $K^0$  in the over-all center-of-mass system.